β-delayed proton decay of a high-spin isomer in ^{94}Ag

I. Mukha,[1,2,*] L. Batist,[3] E. Roeckl,[2] H. Grawe,[2] J. Döring,[2] A. Blazhev,[2,4] C. R. Hoffman,[5] Z. Janas,[6] R. Kirchner,[2] M. La Commara,[7] S. Dean,[1] C. Mazzocchi,[2,†] C. Plettner,[2,‡] S. L. Tabor,[5] and M. Wiedeking[5]

[1]*Instituut voor Kern- en Stralingsfysica, K. U. Leuven, B-3001 Leuven, Belgium*

[2]*Gesellschaft für Schwerionenforschung, D-64291 Darmstadt, Germany*

[3]*St. Petersburg Nuclear Physics Institute, RU-188350 Gatchina, Russia*

[4]*University of Sofia, BG-1164, Sofia, Bulgaria*

[5]*Florida State University, Tallahassee, Florida 32306, USA*

[6]*Warsaw University, PL-00681 Warsaw, Poland*

[7]*Università "Federico II" and INFN Napoli, I-80126 Napoli, Italy*

(Received 4 June 2004; published 19 October 2004)

The decay of the (7^+) and (21^+) isomers of the $N=Z$ isotope ^{94}Ag was studied at the GSI on-line mass separator by measuring β-delayed protons, γ rays, proton-γ and proton-γ-γ coincidences as well as the β-strength distribution. We have observed high-spin (up to $39/2$) states in ^{93}Rh populated by proton emission following the β decay of the ^{94}Ag isomers. The major part of the population is related to the β decay of the known (7^+) isomer whose half-life is 0.61(2) s. The assignment of the high-spin (21^+) isomer in ^{94}Ag with a half-life of 0.39(4) s has been confirmed. The excitation energy and β-decay energy of the (21^+) isomer were measured to be at least 5.4 and 17.7 MeV, respectively. At this excitation energy, the (21^+) isomer is expected to be unbound to direct one-proton, two-proton, or α decays. The remarkably long half-life of the (21^+) isomer with the highest spin and excitation energy ever observed for β-decaying nuclei makes a new textbook example of a nuclear high-spin trap. The branching ratios for β-delayed proton emission are about 20% and 27% for the decays of the (7^+) and (21^+) isomers, respectively. The properties of the experimentally identified ^{93}Rh levels are discussed in comparison to shell-model predictions.

DOI: 10.1103/PhysRevC.70.044311 PACS number(s): 21.10.−k, 21.60.Cs, 27.60.+j

I. INTRODUCTION

Almost all the nuclear-structure properties known to date for $N \simeq Z$ nuclei stem either from in-beam spectroscopy, i.e., the investigation of electromagnetic (γ ray or conversion electron) processes, or from decay studies. The latter experiments generally investigate nuclear disintegrations mediated by strong (direct particle emission), weak (β^+/EC decay), or electromagnetic interactions. The decay of isomers of the $N=Z$ nucleus ^{94m}Ag, which is the topic of this paper, combines all three of these interactions.

By studying the β^+/EC decay of ^{94}Ag, first evidence for a high-spin ($I \geqslant 17$) isomer with a half-life ($T_{1/2}$) of 0.3(2) s in this nucleus, in addition to the known (7^+) isomer [$T_{1/2}=0.42(5)$ s] [1] and (0^+) ground state ($T_{1/2}=29^{+29}_{-10}$ ms) [2], was obtained in a recent experiment [3] performed at the GSI on-line mass separator. In a follow-up measurement, the decay of the two isomers was further studied by improving β-γ-γ coincidence data. This experiment yielded additional information about excited states in the daughter nucleus ^{94}Pd and has allowed to deduce a tentative (21^+) assignment for this spin-gap isomer and to estimate its excitation energy to be about 6.3 MeV [4].

In this paper we present results obtained by investigating both β-delayed γ rays and protons emitted in the decay of the two ^{94}Ag isomers. In view of the comparatively small proton-separation energy in ^{94}Pd and the large Q_{EC} value of ^{94}Ag [estimated to be 4.5(6) MeV and 13.1(6) MeV, respectively, [5]] it is not surprising that β-delayed proton (βp) emission occurs in the decay of ^{94}Ag [1]. However, the detailed proton-γ coincidence data presented in this work are distinctly different from those obtained for other spin-gap isomers, e.g., those occurring in ^{53}Co$(19/2^-)$, ^{95}Pd$(21/2^+)$, or ^{212}Po(18^+) (see review in [4,6]), as these states have lower spin or decay by internal transitions or α emission. One may thus consider the present work to represent an example of an experimental technique which may be called "high-spin spectroscopy using β-delayed protons." The potential of this method is illustrated by the results described in this paper. They concern spin and parity assignments, excitation, and decay energy of the (21^+) isomer as well as high-spin states in ^{93}Rh, populated by proton emission following the β decay of the two (7^+) and (21^+) isomers.

The paper is structured as follows. After introducing the experimental techniques in Sec. II, the results of the positron, proton, and γ-ray measurements are described in Sec. III. Section IV contains a comparison of the experimental results with shell-model calculations, and Sec. V gives a summary and an outlook. Preliminary results of this work have already been presented in the conference contributions [7,8].

II. EXPERIMENT

The ^{94}Ag nuclei were produced in the fusion-evaporation reaction ^{58}Ni(^{40}Ca, $p3n$) by utilizing a 4.8A MeV, 75

*Electronic address: ivan.mukha@fys.kuleuven.ac.be

†Present address: University of Tennessee, Knoxville, TN 37996, USA.

‡Present address: Yale University, New Haven, CT 06520, USA.

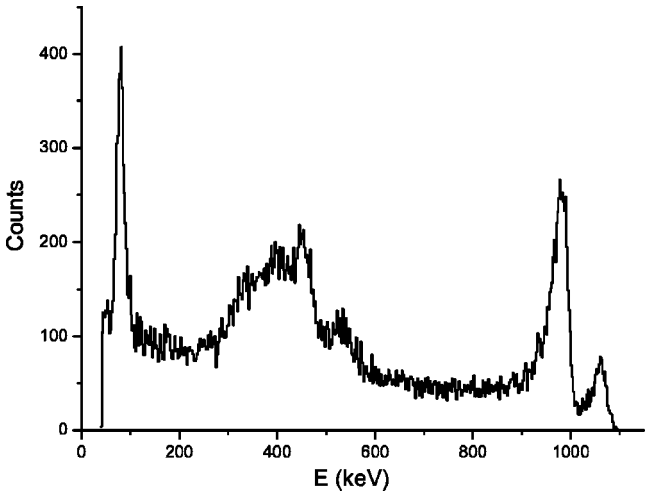

FIG. 1. Energy spectrum obtained in the Si detector for positrons, electrons and x rays emitted in the β^+/EC decay of ^{207}Bi.

particle-nA ^{40}Ca beam from the heavy-ion accelerator UNILAC at GSI. The target consisted of a 2.6 mg/cm^2 thick ^{58}Ni foil enriched to 99.8%. The reaction products were stopped in the FEBIAD-B3C ion source [9,10] with two cold pockets, which suppressed the release of the isobaric ^{94}Pd contamination by a factor of 30 without reducing the ^{94}Ag yield. Singly charged mass-94 nuclei were separated from other reaction products by means of the GSI on-line mass separator [11]. The mass-separated beam of the ^{94}Ag isomers, whose average intensity amounted to about 1.5 atom s^{-1}, was implanted into a tape which removed the activity after preselected time intervals. The implantation point was surrounded by high-granularity arrays of germanium (Ge) and silicon (Si) detectors [7].

Seventeen individual Ge crystals were used for γ-ray detection, with fifteen of them being part of three composite detectors, namely a Cluster [12], two Clover [13], and the remaining two being single Ge detectors. The photopeak efficiency of the Ge array amounted to 3.2% for 1.33 MeV γ rays. This value as well as energy dependence of the detection efficiency were determined by using standard calibration sources. The energy resolution determined as the full width at half maximum (FWHM) of the photopeak was about 3 keV at 1.33 MeV γ-ray energy. Single-hit events in any of the Ge crystals were used to create γ-ray spectra.

The Si array [14], which was used for recording β particles and protons, was positioned inside a cylindrical vacuum chamber with a 1 mm thick aluminum wall. The Si detectors were arranged around the implantation point, covering 65% of 4π solid angle. The array consisted of three individual Si detectors. Each of them had an area of 6 $\times$6 cm^2, was 1 mm thick and had 32 strips with two-channel readouts. The energy response of the Si array measured by using a ^{207}Bi source is illustrated in Fig. 1. The two highest energy peaks are due to *K* and *L* conversion electrons of the 1064 keV transition ($13/2^+ \rightarrow 5/2^-$) in ^{207}Pb. For this radiation, the energy resolution of the Si detector amounted to 25 keV (FWHM). The broad distribution with the bump around 400 keV is due to the conversion electrons which are not stopped in the Si detector (the 99% stopping range of 1 MeV electrons in Si is about 1.7 mm). The structure on the right slope of the 400 keV bump stems from the 570 keV conversion electrons whereas the low-energy peak corresponds to x rays emitted in EC or electron-conversion processes, its FWHM being 10 keV. The observed peaks have been used for an energy calibration. From Fig. 1 one can see that the low-energy detection threshold was about 50 keV. A β-detection efficiency was defined by measuring the conversion electrons in coincidence with the respective γ rays from ^{207}Pb*.

In order to suppress unwanted activity of daughter nuclei, a tape-transport system was used to quickly remove the implanted sources in a stepwise operation. The activity was implanted continuously (grow-in mode) while the tape was at rest. In the period between the end of the implantation interval and the tape movement the decays of the radioactive source were measured as well (decay mode). The grow-in and decay intervals were chosen to be 8.4 and 1.2 s, respectively, which gave a total cycle time of 9.6 s. Data from 3 $\times 10^4$ such cycles were accumulated, corresponding to a total measurement time of 80 h. The β^+/EC-delayed proton decay of ^{94}Ag was measured by recording β-proton, proton-γ, β-proton-γ, and proton-γ-γ events within a coincidence time interval of 100 ns.

In a separate experiment, the β-feeding distributions from the ^{94}Ag decays have been measured with a total absorption spectrometer (TAS) consisting of a large Na I crystal and several auxiliary detectors for detecting $\beta\gamma$, β-proton, proton-γ, and x-ray-γ coincidence events [15]. The TAS setup was almost the same as in the previous measurements of the ^{96m}Ag decays reported in [16] where the TAS setup is described in details. A single Na I crystal with 36 cm length and 36 cm diameter had a cylindrical well in the center, where radioactive sources were periodically transported by using a tape system. The large volume of the crystal allowed a detection of the sum (or total) energy of the γ cascade following β^+, EC, or βp decays with almost 100% efficiency. The total γ energy was measured in sum with the 1024 keV positron-annihilation energy for β^+ decays. Inside the Na I crystal well, the sources were viewed by small β and x-ray detectors from one side, and by ΔE-E proton detector from another side registering β-delayed activity either in coincidence or anti-coincidence with the summed γ rays. With the germanium x-ray detector we could select characteristic x rays from ^{94}Ag obtaining a signature for the EC-decay branch when no γ rays from positron annihilation were registered. The transport-tape time periods consisted of a source collection time of 1.2 s, a source transport time of 0.8 s and a measurement time of 1.2 s. During the measuring time, the next source was being collected on the tape outside TAS. The off-line analysis of the TAS data is described in detail in [16]. The ^{94}Pd contamination of the β-gated ^{94}Ag TAS spectra was measured in a separate experiment with a longer collection time [17], and the TAS spectra from the ^{94}Ag decay were obtained by subtracting the corresponding ^{94}Pd contribution.

III. EXPERIMENTAL RESULTS

In presenting the experimental results obtained in this work, we use the terms "β decay of ^{94}Ag" or "decay of

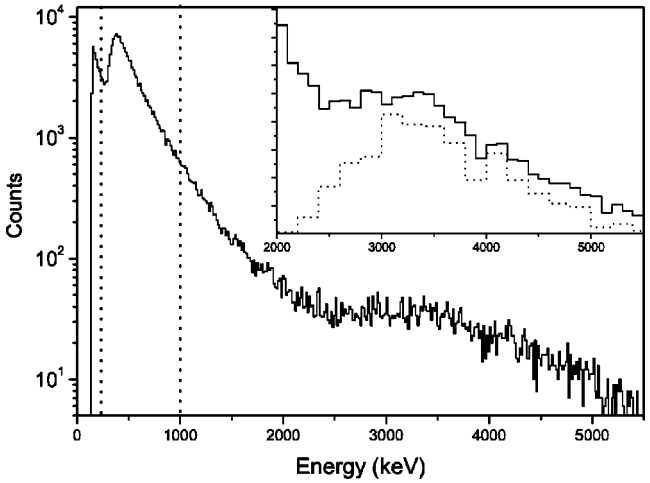

FIG. 2. Spectrum of β particles and protons from the ^{94}Ag decay, measured by the Si array (solid-line histogram). The inset shows the high-energy part of the spectrum together with the βp spectrum of ^{94}Ag measured with ΔE-E telescope in the TAS experiment (dotted-line histogram).

^{94}Ag" for data containing a mixture of the β decays of the (7^+) and (21^+) isomers. Only if individual properties of the isomers are discussed, more specific terms are used.

A. Energy spectra of positrons and protons

The spectrum of charged particles following the β decay of ^{94}Ag is shown in Fig. 2. It has a pronounced peak around 0.5 MeV due to the detection of positrons from β decay. The spectrum falls off exponentially with increasing energy until 2.5 MeV, followed by a broad bump which is centered around 3.5 MeV. This bump is shown in the inset of Fig. 2 in comparison with the spectrum of β-delayed protons from the ^{94}Ag decay as measured in the TAS experiment by using the ΔE-E telescope. As can be seen from this inset, the high-energy part of the spectrum obtained in this work agrees very well with the independently measured βp spectrum of ^{94}Ag in the high-energy part. At low energies, the spectrum of protons measured with the Si array has a low-energy tail in comparison with the ΔE-E spectrum because of energy losses of protons in the collection tape and an admixture of positrons. The optimal proton-positron discrimination energy compromising the large enough proton-detection efficiency (60%) and the relatively small admixture of positrons ($\leqslant$10%) was estimated to be of 1.8 MeV.

B. Energy spectra of γ rays measured in coincidence with positrons and protons

The γ rays observed for mass-94 samples were inspected by using four different coincidence conditions. First, the γ rays were measured in coincidence with particles detected by the Si array, restricting the particle energies (or energy losses) to a range from 0.2 to 1 MeV which is shown in Fig. 2 by the vertical dotted lines. This is the range where β particles dominate. The upper panel of Fig. 3 displays the resulting γ-ray spectrum. Almost all γ rays represent transi-

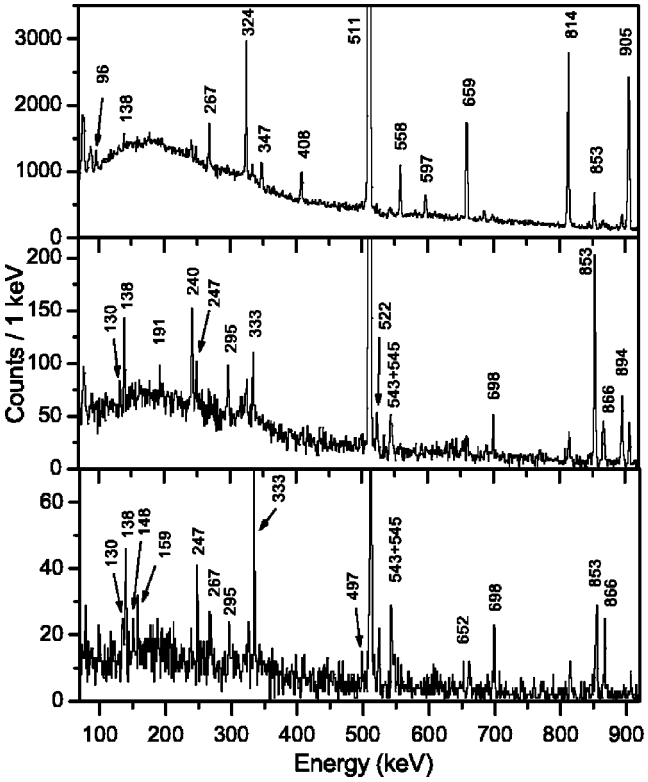

FIG. 3. Energy spectra of γ rays from the ^{94}Ag decay, measured in coincidence with β particles (upper panel), in coincidence with protons (middle panel), and in triple coincidence with protons and one of the intense γ rays of 138, 247, 522, or 698 keV (lower panel). The energies of the strongest transitions in ^{93}Rh, ^{94}Rh, and ^{94}Pd are marked by their energies in keV.

tions in ^{94}Pd, except for the γ ray of 853 keV, which is assigned to known transitions in ^{93}Rh [18]. The corresponding ^{93}Rh state is apparently populated via proton emission following the decay of ^{94}Ag. Furthermore, the spectrum displayed in the upper panel of Fig. 3 shows a peak at 558 keV which is known to be the strongest β-delayed γ ray of ^{94}Pd [19].

The results of the fit of the strongest γ rays observed in the β decay of ^{94}Ag are shown in Table I. The γ-ray energies and intensities are given relative to that of the 814 keV γ line and are used in this work for a normalization purpose. In addition, the γ rays observed in the respective triple β-γ-γ coincidence as well as the half-life values derived for the strongest peaks are listed. The γ-ray energies and intensities shown in Table I agree with the $\beta\gamma$ data analysis reported in [3,4], though the gate condition in the coincident β spectrum is more narrow in our case. Almost all coincident γ rays listed in the last column in Table I are the same as those found in [3,4], and few coincident γ rays are missing which might be related to the different ways of data analysis.

With a second coincidence condition, we selected events that were recorded in the Si array with energies above 1.8 MeV. Such events are estimated to be dominated by β-delayed protons. The resulting γ-ray spectrum changes dramatically, as can be seen from the center panel of Fig. 3. Most of the known γ transitions in ^{94}Pd are not observed any

TABLE I. The strongest γ rays observed in the β decay of ^{94}Ag. Transition energies (E_γ) and intensities (I_γ), half-lives ($T_{1/2}$) and coincident γ lines are given. The I_γ values are normalized to that of the 814 keV line. Coincident γ lines are only listed for the annihilation 511 keV radiation and for transitions in ^{94}Pd but omitted for those in ^{93}Rh and ^{94}Rh.

E_γ (keV)	I_γ (a.u.)	$T_{1/2}$ (s)	Coincident γ lines observed (keV)
267.4(1)	8.7(7)	0.63(5)	(95),324,408,597,659,814,905 979,994,1092,1545
324.0(1)	39.5(15)	0.62(4)	95,347,408,597,659,814,905,994
333.9(7)	5.0(16)		see Table II
408.3(1)	10.8(5)		267,324,597,814,(905),994
511.0(1)	308(7)		all γ lines reported
558.3(1)	20.1(9)		from ^{94}Pd decay
597.1(1)	10.1(11)		267,324,408,814,(905,994),1545
659.4(1)	50.6(18)		(267),324,686,814,905,994
685.8(4)	2.9(12)		659,814
814.0(1)	100(4)	0.61(5)	324,408,597,659,(686),905,979
853.0(1)	8.9(5)		see Table II
905.2(1)	98(4)	0.60(4)	95,324,347,597,659,814,979
978.6(1)	40.7(21)		267,324,814,905
993.7(1)	8.6(7)		95,267,324,408,597,659,1092

longer, while the spectrum is characterized by more than 20 other peaks. They match the γ deexcitation pattern of high-spin states in ^{93}Rh which are known from in-beam γ spectroscopy [18]. Table II lists the γ-ray energies and intensities, obtained from this spectrum, the half-life values deduced from analysis of the γ-ray time characteristics (see Sec. II) as well as coincident γ rays observed in proton-γ-γ coincidence. From the central panel of Fig. 3 one can see that with the high-energy condition applied to the Si array, the intensities of the strongest γ transitions in ^{94}Pd, e.g., those at 324, 659, 814, and 905 keV, decrease by a factor of 60. This illustrates the efficiency of the proton-β discrimination in this work.

In order to further inspect the proton-β discrimination and its relation to the assignments of γ rays, we chose a third, more restrictive coincidence condition, i.e., one that excludes events below 2.5 MeV recorded in the Si array. By comparing the I_γ values deduced from this spectrum with those listed in Table II, we conclude that the β contribution to the high-energy region of the Si spectrum is only about 5×10^{-3} of the total intensity found for events with energies beyond 1.8 MeV. For the data analysis presented below, we accepted the E_γ and I_γ values derived from the Si events above 1.8 MeV, except for the case of the 698 and 866 keV lines (see Table II). These data are in quantitative agreement with those derived by using the 2.5 MeV threshold which provides more accurate data for a few γ rays, i.e., for those at 191 and 1494 keV (see Table III).

As we have observed the feeding of many highly excited states in ^{93}Rh, populated by proton emission from excited states of ^{94}Pd, an analysis of the proton-γ-γ coincidences was performed in order to establish the γ deexcitation cascades between ^{93}Rh levels. As an example for this analysis, the lower panel of Fig. 3 displays the γ coincidence spectrum obtained from triple-coincidence proton-γ-γ events. This spectrum was obtained by using a fourth coincidence condition. The latter was defined by selecting single-hit events in any of the 17 Ge crystals that were coincidental with (i) Si-detector events above 1.8 MeV and (ii) 138, 247, 522, or 698 keV γ rays detected in any of the remaining 16 Ge crystals. The first column of Table II lists γ rays, which are assigned to represent transitions in ^{93}Rh on the basis of the half-life data (see third column of Table II) and a comparison of the positron-γ and proton-γ spectra (see upper and central panel of Fig. 3). The proton-γ-γ coincidence data (see fourth column of Table II) reveal further ^{93}Rh transitions, namely those at 148, 163, (273), 297, 382, 440, 546, 557, 570, 622, 654, 680, 695, 842, and 948 keV (parentheses indicate tentative assignments). Some of these transitions were observed by using in-beam γ spectroscopy [18], others are tentatively assigned because of matching the established energy levels in ^{93}Rh.

C. Excited states in ^{93}Rh populated in β decay

Table III lists the experimental properties of ^{93}Rh levels, assigned on the basis of the proton-γ and proton-γ-γ coincidence data discussed above. Figure 4 displays the corresponding level scheme of ^{93}Rh. It comprises all γ rays listed in the first column of Table II, except the weak high-energy γ rays at 1565 and 1861 keV which are not placed in the ^{93}Rh level scheme.

The non-yrast levels are partially taken from data on the β decay of ^{93}Pd [20], while the yrast-band assignments are adopted according to [18]. The 853 and 5447 keV levels are the only exceptions from this procedure. On the basis of the larger intensity of the 853 keV γ line relative to that of the 866 keV one, we conclude that these two transitions must be inverted in comparison with the earlier assignment [18]. The analogous conclusion is drawn for the 5447 keV state on the basis of the relative intensities of the 247 and 698 keV γ lines. We interpret three weak γ lines at 191, 130, and 148 keV, observed in addition to those found earlier [18], as being members of the odd-parity band (see lower panel of Fig. 3). As they have very small intensities, we have tentatively placed them on top of the 6389 keV level. If there were any further higher-energy γ transitions from higher-lying ^{93}Rh states populated by βp emission, they are apparently below the sensitivity limit of the present measurement. Furthermore, we have observed weak γ rays at 368, 382, 440, 622, and 705 keV which were found to be coincidental with protons and 511 keV γ rays only (see Table II). From a previous study of the ^{93}Pd β decay, the 622 and 382 keV lines have been assigned to depopulate the $5/2^+$ level of ^{93}Rh [20]. As other lines have not been seen in coincidence with γ rays from ^{93}Rh, we could not place them in the ^{93}Rh level scheme, and therefore did not list them in Table III.

The high-spin levels of ^{93}Rh fed in βp decay give further evidence for the (21^+) isomer in ^{94}Ag identified in [3,4]. Its spin can be estimated by inspecting the highest-spin levels

TABLE II. Gamma rays for the decay of ^{94}Ag, observed in coincidence with proton events above 1.8 MeV and assigned as transitions in ^{93}Rh. Notifications and normalization are the same as in Table I. All γ rays listed were found to be in coincidence with 511 keV γ-rays.

E_γ (keV)	I_γ (%)	$T_{1/2}$ (s)	Coincident γ lines observed (keV)
130.2(3)	0.4(2)		138,295,333,543,546,853,866
137.6(1)	1.0(2)	0.45(8)	191,247,295,333, 522,543,546,653, 695,698,853,866,(1494)
159(1)	0.4(2)		297,543,546,853,(866)
191.2(2)	0.4(2)		138,148,247,295,(333), 522,543,546,853
240.1(1)	2.0(2)	0.56(9)	557,570,654,680,842,1390
246.9(1)	0.7(1)	0.46(14)	138,148,159,(191),333,(497), 522,544,695,698, 853,866,(1494)
295.4(2)	1.0(2)	0.64(21)	138,163,247,297,333,497, 543,546,653,(695),853,866,(1362)
333.4(1)	1.75(16)	0.56(14)	130,138,163, 247,295,497,522, 543,546,698,853, 866,948,1362,1494
382(1)	0.3(2)		–
496.9(3)	0.37(10)		(273,295,333),543,(698),853
511.03(3)	46.4(10)	0.52(5)	130,138,(159),191,240, 247,295,(297),333,368,382, 440,522,543, 622,653,698, 853,866,894,1362,1494
522.4(1)	0.92(13)	0.46(16)	130,138,247,333, 543,546,698, 853,866
543.7(2)[a]	2.4(2)	0.30(13)	130,138,247,333,497, 522,543,546, 698,853,866,(1494)
622(1)	0.5(3)		–
652.5(2)	0.56(13)		138,(240),295,333,546
698.0(1)	1.64(19)	0.25(11)[b]	138,247,333,522,543,853,866
852.9(1)	11.3(5)	0.68(10)	138,247,333,522,543,698,866
866.0(1)	3.24(16)	0.50(14)[b]	138,247,333,522,543,698,853
894.2(1)	4.3(2)	0.48(12)	(333),557,570
1361.7(3)	0.36(12)		247,(295),333
1451.0(7)	0.41(13)		–
1463.7(8)	0.43(17)		–
1493.8(5)	0.7(3)		138,247,333,522
1565.4(4)	0.50(17)		–
1718.4(5)	0.7(2)		–
1861.0(3)	0.53(16)		–
2197.8(5)	0.88(16)		–

[a]Line interpreted as a doublet consisting of the 542.8 and 545.5 keV γ rays (Ref. [18]).
[b]Half-life deduced by using a restrictive proton-coincidence condition.

TABLE III. Level energies, spins, and parities of ^{93}Rh states, respective γ-ray energies, apparent total probabilities of level population per ^{94}Ag decay (P_i), and apparent β-feeding intensities ($I_{\beta p}$) observed in β-delayed proton decay of ^{94}Ag.

E_{level} (keV)	I^{π}	E_{γ} (keV)	P_i(%)	$I_{\beta p}$(%)
0.0	$(9/2^+)$	-	21(2)[a]	3.3(7)[a]
240.1(1)	$(7/2^+)$	240.1(1)	1.7(2)	1.7
622(1)	$(5/2^+)$	622(1)	0.4(3)	0.4
852.9(1)	$(13/2^+)$	852.9(1)	9.6(4)	6.8
894.2(1)	$(11/2^+)$	894.2(1)	3.1(2)	3.0
894.2(1)	$(11/2^+)$	654(1)	$\leqslant$0.2	?
1451.0(7)	$(7/2^+)$	1451.0(7)	0.3(1)	0.3
1451.0(7)	$(7/2^+)$	557(1)	$\leqslant$0.2	?
1463.7(8)	$(13/2^+)$	1463.7(8)	0.36(15)	0.3
1463.7(8)	$(13/2^+)$	570(1)	$\leqslant$0.2	?
1630(1)	$(9/2^+)$	1390(1)	$\leqslant$0.2	?
1718.4(5)	$(11/2^+)$	1718.4(5)	0.5(2)	0.5
1718.9(1)	$(17/2^+)$	866.0(1)	2.8(2)	1.3
2052.3(2)	$(21/2^+)$	333.4(1)	1.5(1)	0.0
2197.8(5)	$(5/2^+)$	2197.8(5)	0.7(2)	0.7
2595.1(2)	$(23/2^+)$	542.8[b]	1.5(3)[c]	0.3
2890.5(3)	$(25/2^+)$	295.4(2)	0.9(1)	0.2
3543.0(4)	$(25/2^+)$	652.5(2)	0.5(1)	0.1
3543.0(4)	$(25/2^+)$	948(1)	$\leqslant$0.2	?
4088.7(3)[d]	$(27/2^+)$	545.5[b]	1.3(5)[e]	0.1
4088.7(3)[d]	$(27/2^+)$	1493.8(3)[f]		
4252.2(5)	$(29/2^+)$	1361.7(3)	0.3(1)	0.0
4549.4(5)	$(31/2^+)$	297.2[b]	$\leqslant$0.2	?
4708.4(11)	$(33/2^+)$	159(1)	0.4(3)	0.3
4611.1(4)	$(25/2^- - 29/2^-)$	522.4(1)	1.7(1)	?
4748.9(4)[g]	$(27/2^- - 31/2^-)$	137.6(1)	2.0(2)[h]	0.1
4748.9(4)[g]	$(27/2^- - 31/2^-)$	496.9(3)		
5446.9(5)	$(29/2^- - 35/2^-)$	698.0(1)	1.4(2)	0.8
5693.8(5)	$(31/2^- - 39/2^-)$	246.9(1)	0.6(1)	0.6
6388.5(6)	$(33/2^- - 43/2^-)$	694.7[b]	$\leqslant$0.2	?
6579.7(6)	$(35/2^- - 47/2^-)$	191.1(1)[f]	0.4(2)	0.4
6709.9(7)[i]	$(37/2^- - 47/2^-)$	130.2(3)	0.4(2)	0.4
6858(1)[i]	$(39/2^- - 47/2^-)$	148(1)	$\leqslant$0.2	?

[a]Intensity of the β-delayed proton decay into the ^{93}Rh ground state is deduced from the TAS measurements.
[b]Value is adopted from (Ref. [18]).
[c]Derived by assuming $I_\gamma(333) > I_\gamma(543) > [I_\gamma(295) + I_\gamma(1494)]$.
[d]Average value of the two experimental level energies 4088.5(4) and 4088.9(4) keV.
[e]Derived by assuming $I_\gamma(546) = I_\gamma(543+546) - I_\gamma(543)$.
[f]Line positions and intensities are deduced by using the coincident-proton threshold of 2.5 MeV.
[g]Average value of the two experimental level energies 4748.7(4) and 4749.1(5) keV.
[h]Both γ de-excitation and internal conversion are taken into account.
[i]Tentative assignment.

observed in ^{93}Rh. Assuming a $(39/2^-, 47/2^-)$ spin-parity range for the highest level placed at 6858 keV, we obtain $I \geqslant 18$ for the proton-emitting state in ^{94}Pd, and hence $I \geqslant 17$ for the ^{94}Ag isomer (assuming allowed β decay). This estimate is based on the assumption that the spin-parity changes ($\Delta I^{\Delta\pi}$) between parent and daughter states respective to those of parent states are 1^{no} and $3/2^{yes}$ for β decay and proton emission, respectively. This estimate agrees with that obtained earlier [3].

D. Branching ratios for β-delayed proton emission

On the basis of the measured γ-ray energies and intensities and the respective ^{93}Rh level assignments, we can esti-

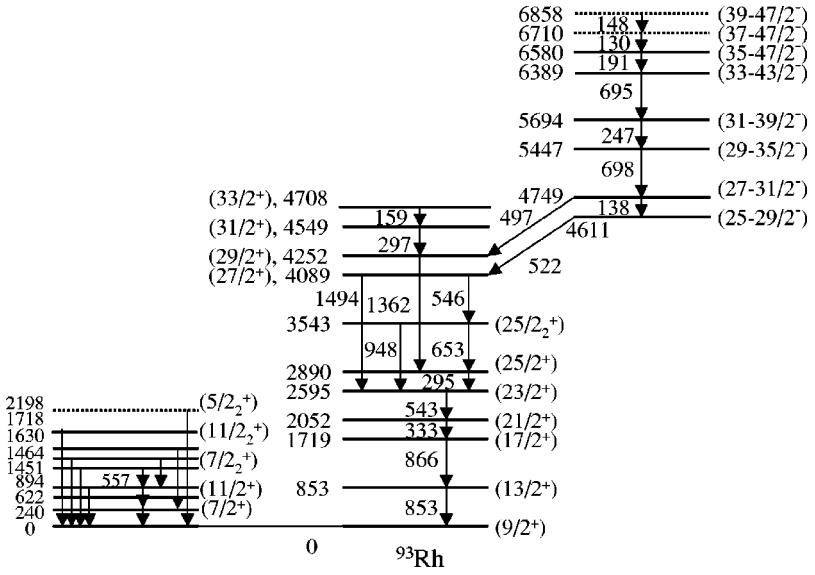

FIG. 4. States in ^{93}Rh populated in β decay of ^{94}Ag via emission of delayed protons. Two yrast bands of γ transitions between levels with even and odd parity are shown in the center and on the right, respectively. Low-energy states which are not associated with yrast bands are shown on the left. Level and γ-ray energies are given in keV. Their accuracy is between 0.1 and 1.1 keV. Tentative spin-parity assignments are shown in parenthesis.

mate the branching ratios for βp emission from both isomers in ^{94}Ag. We assume that the isomers decay into ^{94}Pd$+\gamma$ and ^{93}Rh$+$p$+\gamma$ channels only, disregarding possible direct charged-particle emissions and internal transitions of the ^{94}Ag isomers. Therefore the sum $I_{\mathrm{Pd}}(7^+)+I_{\mathrm{Rh}}(7^+)+I_{\mathrm{Pd}}(21^+)+I_{\mathrm{Rh}}(21^+)$ should be 100% per one decay of ^{94}Ag, where $I_{\mathrm{Pd,Rh}}(7^+,21^+)$ are the respective β intensities, i.e., $I_{\mathrm{Rh}}=\Sigma I_{\beta p}$. In such a case all the β intensities listed in Table II should be renormalized by using the additional condition that the 814 keV state in ^{94}Pd is a "collector" state fed by all β transitions and subsequent γ rays except for 10% of intensity resulting in conversion electron decays [3,4]: $I_{\mathrm{Pd}}(7^+)+I_{\mathrm{Pd}}(21^+)=1.1\cdot I_{\gamma}(814\ \mathrm{keV})$. The derived partial branching values, $I_{\beta p}$, are listed in Table III. One should note, that the intensity of the β-delayed proton decay into the ^{93}Rh ground state was derived from the TAS-experiment data by selecting the protons coincident with the 1022 keV γ peak due to β^+ annihilation in TAS. The relative intensity of this decay branch has been measured to be $0.16(3)\cdot\Sigma I_{\beta p}$. In this case, we have assumed $P_i(\mathrm{Rh}_{g.s.})=I_{\mathrm{Rh}}$.

The proton branching ratios can thus be calculated for each of the two isomers from the intensities of the decays connected to proton emission. For this purpose, the respective intensities from Table II are used, e.g., $b_p(21^+)=I_{\mathrm{Rh}}(21^+)/[I_{\mathrm{Rh}}(21^+)+I_{\mathrm{Pd}}(21^+)]$. A further assumption is that βp emission from the (7^+) isomer occurs predominantly with angular momenta $\leqslant 3/2$, thus feeding states in ^{93}Rh with $I\leqslant 19/2$ only. Hence, the feeding of the higher-spin states of ^{93}Rh is entirely assigned to the decay of the (21^+) isomer. The corresponding intensities $I_{\mathrm{Rh}}(7^+)$ and $I_{\mathrm{Rh}}(21^+)$, derived from Table III, amount to 18% and 3%, respectively. Furthermore, γ rays following a β feeding of ^{94}Pd excited states with $I^{\pi}\leqslant 8^+$ are assigned to the decay of the (7^+) isomer only [3,4]. By using the ^{94}Pd level scheme [3,4] and its γ-ray intensities listed in Table I, we estimate the $I_{\mathrm{Pd}}(7^+)$ and $I_{\mathrm{Pd}}(21^+)$ values to be 72% and 8%, respectively. Finally, the βp branching ratios are estimated to be about 20% and 27% for the decays of the (7^+) and (21^+) isomers, respectively. Using the estimate of the quantity $I_{\mathrm{Pd}}+I_{\mathrm{Rh}}$, the relative contribution of the ^{94}Ag isomers to the mass-separated $A=94$ beam are found to be 89% and 11%, respectively.

A remarkable feature of the observed βp-decay pattern is the preferred feeding of odd-parity states at high excitation energies in ^{93}Rh, which points to odd orbital momenta of the emitted protons when assuming even parity for the ^{94}Pd parent states [3]. Such a feature may be qualitatively explained via a simplified structure of the (21^+) isomer of ^{94}Ag and its high-spin β-daughters (20^+-22^+) in ^{94}Pd within the restricted $(p_{1/2},g_{9/2})$ model space (see Sec. IV). The spin-parity range, which can be populated in odd-parity states of ^{93}Rh by emission of a $p_{1/2}$ proton from ^{94}Pd*, is $(39/2^-$ to $45/2^-)$. For the even-parity states in ^{93}Rh, the spin range that can be reached via an emission of a $g_{9/2}$ proton is $(31/2^+$ to $53/2^+)$. The barrier penetration is easiest for the highest decay energies and therefore a population of the lowest spin states in the two ranges is preferable. Moreover, the centrifugal barrier favors $\ell_p=1$ over $\ell_p=4$ emission, which cannot be compensated by the higher decay energy (or lower excitation energies in the ^{93}Rh daughter) for the $\ell_p=4$ case. Thus the odd-parity states in ^{93}Rh are populated up to much higher spin and excitation energy and more strongly than the even-parity states, in agreement with the observed branching ratios, see Table III.

E. Estimates of the Q_{EC} values of the ^{94}Ag isomers

We estimated the Q_{EC} values of the isomers in ^{94}Ag by three independent methods. The first one is based on determining the maximum energies (end-points) of the proton spectra obtained in coincidence with known γ-ray transitions in ^{93}Rh. Figure 5 shows six energy spectra of β particles and protons measured with the Si array in coincidence with different γ transitions assigned to ^{93}Rh. All spectra are characterized by a broad bump at an energy around $2-3$ MeV corresponding to protons, and a low-energy peak corresponding to β particles. The end points of the bumps assigned to protons are in the range from 5.5 to 6.1 MeV. These values were used to estimate the highest ^{94}Pd excitation energy populated by βp decay of the ^{94}Ag isomers by using the relation

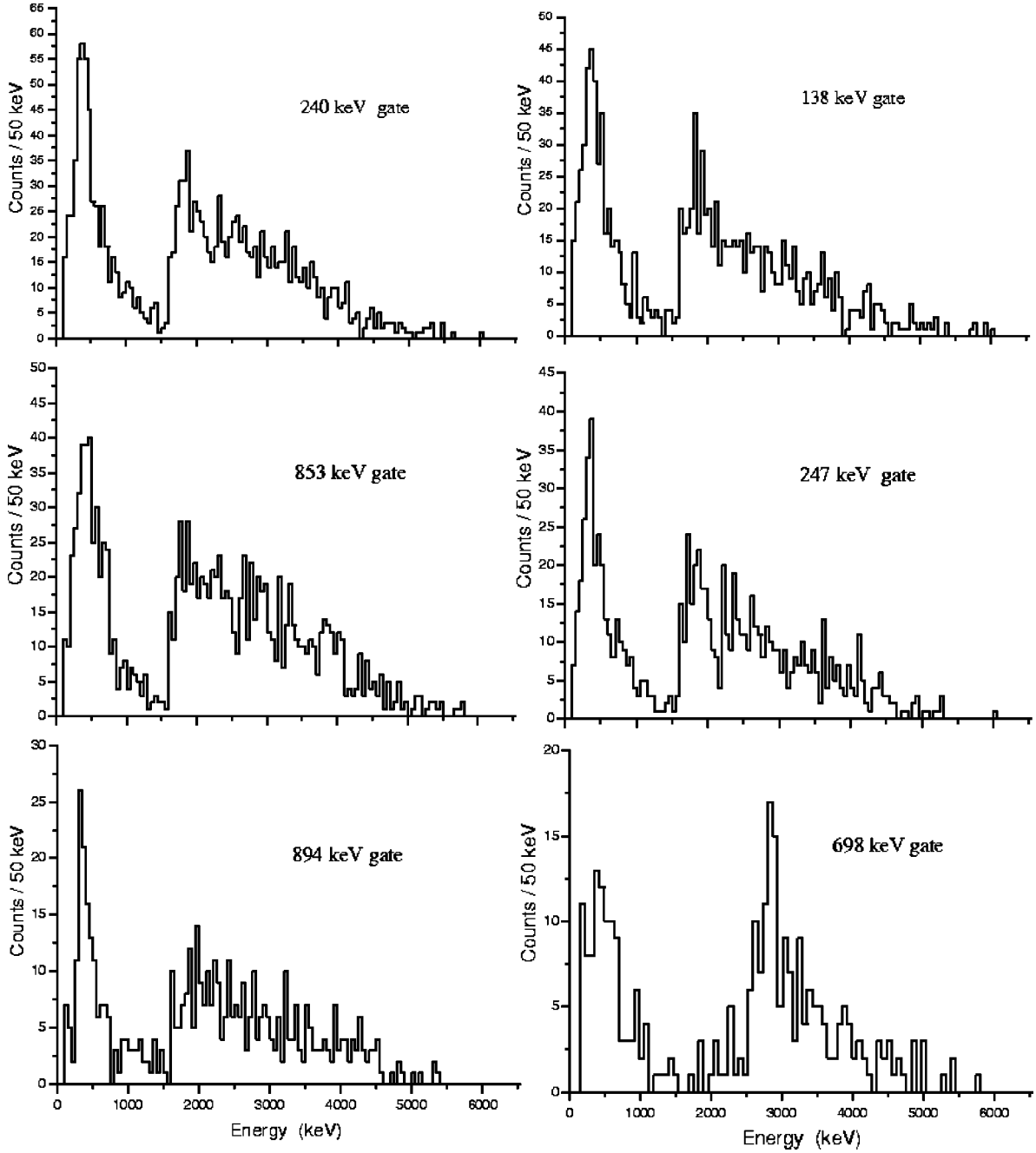

FIG. 5. Proton and positron spectra measured in coincidence with γ rays depopulating excited states of ^{93}Pd. The γ lines used for the coincidence gating are indicated for each spectrum.

$E(^{94}\mathrm{Pd}^{*})=S_p+E_p+E(^{93}\mathrm{Rh}^{*})$, where S_p is the proton separation energy in ^{94}Pd, E_p the proton energy, and $E(^{93}\mathrm{Rh}^{*})$ the excitation energy of the ^{93}Rh level populated by proton emission. For example, the 698 keV γ transition indicates a population of the 5447 keV, $(29/2^{-},35/2^{-})$ state in ^{93}Rh, thus excluding γ-ray emission after βp decay of the (7^{+}) isomer in ^{94}Ag (see Fig. 4). As the proton separation energy in ^{94}Pd is estimated to be 4.5(6) MeV [5], the end-point value of 5.5 MeV of the respective proton spectrum corresponds to a value of at least 15.4 MeV for the highest excitation energy of ^{94}Pd states populated in β decay of the (21^{+}) isomer in ^{94}Ag. Similar estimates made for the 138 and 247 keV γ-gated proton spectra, shown in Fig. 5, yield maximum $E^{*}(^{94}\mathrm{Pd})$ values of 15.3 and 15.5 MeV, respectively. For the decay of (7^{+}) isomer, $E(^{94}\mathrm{Pd}^{*})$ estimates of 10.3 and 10.7 MeV were obtained in a similar way by using the 240 and 894 keV γ-gated proton spectra, respectively (see Fig. 5). Thus the Q_{EC} values of the (7^{+}) and (21^{+}) isomers in ^{94}Ag should be at least 12.0 and 16.8 MeV, respectively, assuming that the measured protons follow a positron emission whose minimum energy is larger than the detection threshold of 0.3 MeV [i.e. $Q_{EC}\geqslant E(^{94}\mathrm{Pd}^{*})+1.022+0.3$ (MeV)].

The excitation spectrum of ^{94}Pd states populated in β decay of ^{94}Ag which are followed by a proton emission into

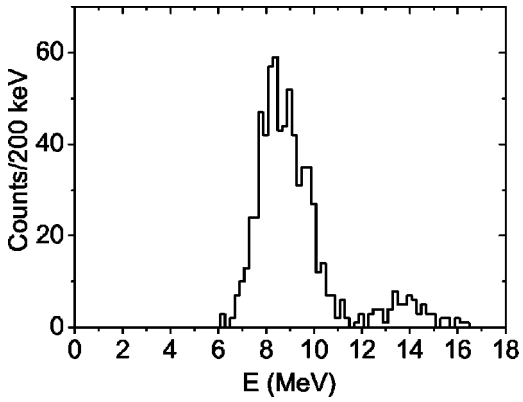

FIG. 6. Spectrum of ^{94}Pd intermediate states populated in βp decay of ^{94m}Ag. The excitation energy $E(^{94}\mathrm{Pd}^{*})$ is a sum $E_\gamma + E_p + S_p$ of the γ and proton energies (measured with the TAS and proton detectors) and the proton separation energy in ^{94}Pd.

^{93}Rh excited states has been measured by operating TAS in coincidence with protons registered by its auxiliary Si detectors. The measured $E(^{94}\mathrm{Pd}^{*})$ distribution is shown in Fig. 6, where one can clearly see two bumps whose positions and intensities can be explained in a consistent way as being due to decays of the (7^+) and (21^+) isomers in ^{94}Ag. By inspecting the high-energy part of the $E(^{94}\mathrm{Pd}^{*})$ spectrum which ends at 16.4 MeV (see Fig. 6), we have a second method to estimate the Q_{EC} value of the (21^+) isomer. With the assumption described above $[Q_{EC} \geqslant E^{*}(^{94}\mathrm{Pd}) + 1.022 + 0.3\ (\mathrm{MeV})]$, the $Q_{EC}(21^+)$ value is found to be larger than 17.7 MeV. Finally, the low-limit Q_{EC} value related to the (21^+) isomer is estimated to be 17.7 MeV. A close inspection of the β-strenth distributions derived on the basis of the excitation spectrum of ^{94}Pd shown in Fig. 6 will be done in a separate publication [21].

As can be seen from the comparatively modest intensity of the β component of the spectra displayed in Fig. 5, the EC component of β decay represents an important part of the processes preceding the proton emission. Therefore the third way of estimating the Q_{EC} value is based on the relative weights of the β^+ and EC decay branches of isomers in ^{94}Ag. The weights were determined by using again the β^+/EC-delayed proton spectra gated by known γ rays. For this purpose we assumed that (i) the β decay of ^{94}Ag into a highly excited state in ^{94}Pd proceeds by a Gamow-Teller transition via two competing channels, a β^+ emission or an EC decay; (ii) the ^{94}Pd level under consideration deexcites by a proton emission into excited states in ^{93}Rh, and (iii) the latter emit γ rays. Thus the intensities of β^+ and EC processes can be defined from the β-proton-γ and proton-γ data, respectively. The theoretical dependence of the β^+/EC ratio on β-decay energy, E_β, was taken from [22], and the Q_{EC} value of the (21^+) isomer of ^{94}Ag was then determined as the sum $Q_{EC} = E_\beta + E(^{94}\mathrm{Pd}^{*}) + 1.022$ (MeV). For example, for the case of a β transition followed by emission of 2.9 MeV protons and 698 keV γ-rays (see the respective proton peak in Fig. 5), the $E(^{94}\mathrm{Pd}^{*})$ value is found to be 12.9 MeV by using the level assignment shown in Fig. 4. The corresponding β^+/EC ratio is 1.5(4), which yields $E_\beta = 1.7(2)$ MeV and thus $Q_{EC} = 15.6(2)$ MeV. Actually, this estimate represents a lower limit, as the 5447 keV state in ^{93}Rh, which deexcites by the 698 keV γ ray, can be populated also from higher-lying states in ^{93}Rh, e.g., those emitting the 695 or 191 keV γ rays. We thus conclude that the obtained upper-limit Q_{EC} estimate of 15.6(2) MeV for the (21^+) isomer does not contradict the corresponding value of 17.7 MeV described above.

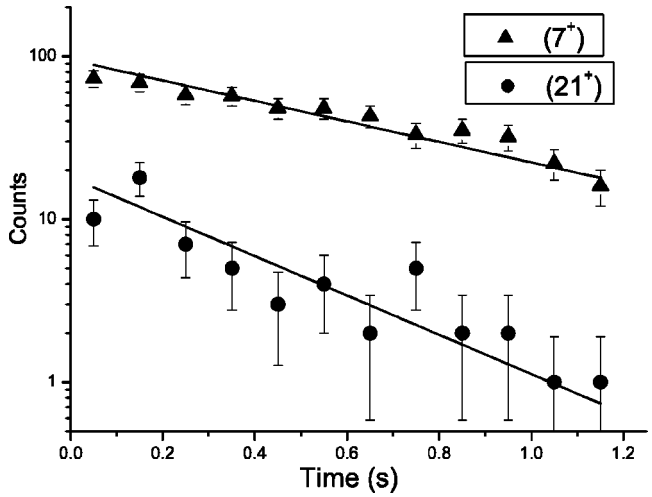

FIG. 7. Time dependence of the β-proton-TAS coincidences measured with the TAS and proton detectors in decays of ^{94m}Ag. The solid lines are the results of data fit.

A similar Q_{EC} estimate has been applied to the TAS data, where we could distinguish two βp transitions only, into the ground state and the 853 keV excited state in ^{93}Rh, which are mainly populated by decay of the (7^+) isomer in ^{94}Ag, see Table III. In the first case we have measured the β^+/EC ratio for the protons detected in coincidence with the 1022 keV peak in the TAS spectrum and in anticoincidence with TAS, respectively. The obtained β^+/EC ratio of 15.6^{+7}_{-4} corresponds to $E_\beta = 5.10(45)$ MeV. The average proton energy (calculated as the position of the peak in the proton spectrum, see dotted-line histogram in Fig. 2) for this case was 3.49 MeV, and thus $Q_{EC} = 5.10(45) + 3.49 + 4.47 = 13.09(45)$ MeV. In the second case, the β^+/EC ratio of protons detected in coincidence with the 853 keV peak in the TAS spectrum and in coincidence with the (1022+853) keV peak in TAS, respectively, yielded $E_\beta = 4.25(40)$ MeV. The average proton energy is 3.37 MeV, and thus $Q_{EC} = 4.25(40) + 3.37 + 4.47 + 0.853 = 12.95(40)$ MeV. Therefore, the $Q_{EC}(7^+)$ value, deduced by averaging the results from all three methods, is of 13.0(3) MeV.

The excitation energy of the (21^+) isomer in ^{94}Ag may be deduced by using the above-mentioned Q_{EC} estimates. On the basis of the shell-model prediction of 0.66 MeV for the excitation energy of the (7^+) isomer [3], we conclude that the excitation energy of the (21^+) isomer is of the order 5.4 MeV. This lower limit is in qualitative agreement with the value of 6.3 MeV, deduced from a comparison with shell-model predictions [4].

F. Beta decay half-lives

The half-life values of both ^{94}Ag isomers were obtained by fitting the time distributions of the activity measured with

the high-resolution and the TAS setups. In the high-resolution experiment, the time distributions were measured both in "grow-in" and "decay mode" (see Sec. II). Single-component exponential decay and grow-in functions were used for a maximum-likelihood fit of the data. The fit results are listed in Tables I and II for the most intense γ lines observed in coincidence with protons and β particles, respectively. In the TAS experiment, the time distributions of the ^{94m}Ag decays were measured with the TAS and proton detectors in a decay mode, and they are shown in Fig. 7. The data are selected from the measured β-proton-TAS coincidences. The triangles correspond to data obtained for (7^+) isomer decays by demanding that the excitation energy of the daughter ^{94}Pd states $E(^{94}\mathrm{Pd}^*)$ is less than 12 MeV (see Fig. 6). The filled circles correspond to the decay of the (21^+) isomer. They were selected with the condition $E(^{94}\mathrm{Pd}^*)>12$ MeV (see Fig. 6). The maximum-likelihood fits of the data give half-life values of 0.61(7) s and 0.30(6) s for the decays of the (7^+) and (21^+) isomers, respectively.

Discussion of the half-life of the (7^+) *isomer*. In the high-resolution experiment, the half-life of the (7^+) isomer has been derived on the basis of the most intense γ transitions in ^{93}Rh whose spin is $17/2$ or lower (see data for the 853, 866, 240, and 894 keV γ lines in Table II), by assuming that these states are mainly populated via emission of $\ell=0$, 2 protons from $I^\pi \leqslant 8^+$ states in ^{94}Pd which are predominantly populated in β decay of the (7^+) isomer. Contributions from the (21^+) isomer may be neglected because of its relatively low production, see Sec. III D. The statistically weighted average value of the half-life is then $T_{1/2}(7^+)=0.57(6)$ s. This value differs from the previous value of 0.36(3) s derived from a grow-in measurement [3]. Such a difference can tentatively be explained by a systematic uncertainty that has been disregarded when deriving half-lives from a grow-in measurement only. For example, we reproduce the half-life value from [3] if we fit only part of the present time distribution corresponding to the grow-in mode. For a cross-check, the half-life value of the (7^+) isomer of ^{94}Ag has been derived on the basis of the time dependence of the most intense γ transitions in the ^{94}Pd daughter (see data for the 814, 905, 267, and 324 keV γ lines in Table I). This method yields a statistically weighted average value of $T_{1/2}(7^+)=0.62(3)$ s in agreement with the result of 0.59(2) s [4] obtained by analyzing β-coincident γ transitions in ^{94}Pd with a different β-gate condition (see Sec. III A). Both these values agree with the result 0.61(7) s obtained for the isomer (7^+) in decay mode by using the total absorption spectrometry. All in all, we recommend the half-life value $T_{1/2}(7^+)=0.61(2)$ s, derived as a statistically weighted average of the $\beta\gamma$, $p\gamma$, and TAS data of this work.

Discussion of the half-life of the (21^+) *isomer*. In the high-resolution experiment, the half-life of the (21^+) isomer was determined by using several intense γ transitions in ^{93}Rh which cannot be populated via β decay of the (7^+) isomer (see Table II). On the basis of the assumed decay scheme, the proton-coincident γ lines at 138, 247, 295, 333, 522, 698, and 543 keV were chosen for this purpose, yielding a statistically weighted average value of 0.42(5) s, which agrees with the previous value of 0.3(2) s [1] within the respective experimental uncertainties. The new half-life value (reported preliminarily in [7]) is confirmed by the analysis of β-coincident γ transitions in ^{94}Pd [4] [$T_{1/2}=0.47(8)$ s], and also agrees with the value of 0.30(6) s measured in decay mode by means of the TAS. Therefore we recommend the half-life value $T_{1/2}(21^+)=0.39(4)$ s, derived as a statistically weighted average value of all mentioned results. We expect that the present values, being derived from both grow-in and decay data, are more accurate than those found in the grow-in measurement only [3].

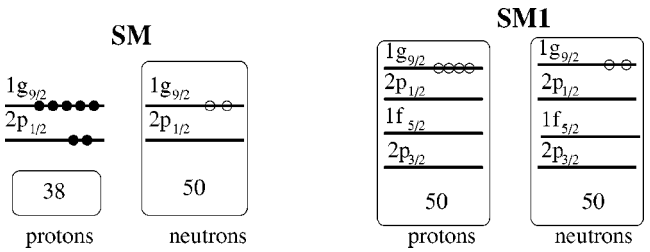

FIG. 8. Single-particle shell-model orbitals used in calculations of ^{93}Rh states. The SM configurations applied with the empirical Gross-Frenkel residual interaction (Ref. [24]) are shown on the left panel. The SM1 orbitals used with the interaction of Sinatkas *et al.* (Ref. [26]) are shown on the right panel: The active particle (•) and hole (◦) occupation is indicated for the leading ground-state configuration.

IV. SHELL-MODEL CALCULATIONS AND DISCUSSION

The experimental levels in ^{93}Rh have been compared with shell-model calculations of two types. The first calculation, labeled "SM," has been performed with the code OXBASH [23] considering protons and neutron holes within the $(p_{1/2},g_{9/2})$ single-particle orbitals shown on the left panel of Fig. 8. The empirical residual interaction derived by Gross and Frenkel from ten nuclei with $N=48-50$ [24] has been used. The second calculation, denoted "SM1," has been performed with the shell-model code ANTOINE [25] by using the interaction parameters of Sinatkas *et al.* [26] who assumed a ^{100}Sn inert core and considered proton and neutron holes distributed in the $g_{9/2}$, $p_{1/2}$, $p_{3/2}$, and $f_{5/2}$ orbitals as shown in Fig. 8 on the right panel.

Most of the states in ^{93}Rh populated by βp emission can be explained as even-parity yrast states by using simple $\pi(p_{1/2},g_{9/2})^6\nu g_{9/2}^{-2}$ configurations in shell-model calculations.

In Fig. 9, the even-parity states in ^{93}Rh derived from the γ rays coincident with β-delayed protons (left panel) in the present work and partly known from previous study [18] are compared with the results of SM and SM1 shell-model calculations. One can see that both types of calculations reproduce well the data up to high excitation energy and spin values.

A comparison for the odd-parity states in ^{93}Rh is hampered by the fact that experimentally only tentative spin assignments are made for these states [18]. Therefore a conclusive interpretation cannot be given. In Fig. 10, the observed ^{93}Rh levels are compared with the results of SM and SM1

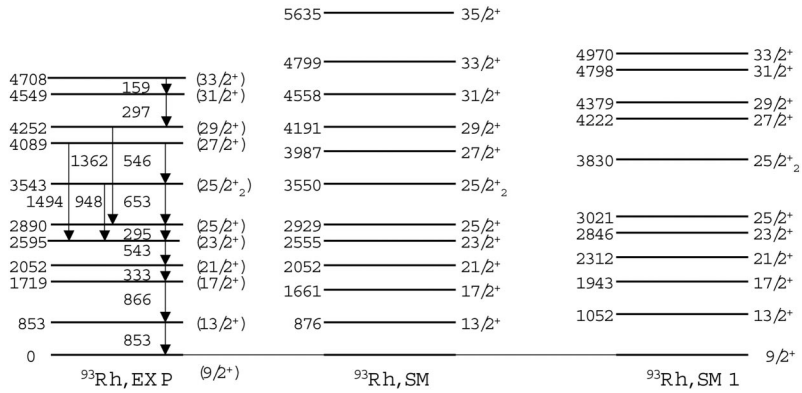

FIG. 9. Even-parity yrast states in ^{93}Rh predicted by the shell-model calculations SM and SM1 (see center and right panels, respectively) in comparison with the experimental scheme derived from the γ rays observed in β decay of ^{94}Ag in coincidence with delayed protons (left panel). Energies of the states and γ rays are given in keV.

shell-model calculations. One can see that the simple $(p_{1/2}, g_{9/2})$ configuration space fails to reproduce the right order of high-spin yrast states. The application of the $g_{9/2}$, $p_{1/2}$, $p_{3/2}$, and $f_{5/2}$ space improves the situation though a quantitative description of the data is still to be achieved.

We have made tentative spin-parity assignments to some low spin and low excitation energy non-yrast states in ^{93}Rh, which have been derived from a comparison of the experimental scheme, established on the basis of β-proton-γ data and the results of shell-model calculations, e.g., the SM calculations presented in the right panel of Fig. 11. These states do not belong to the main yrast cascades as most of them are bypassed by the deexcitation of the 853 keV state to the ground state of ^{93}Rh. An interesting feature of the ^{94}Ag decay is the much weaker β feeding of the $(5/2^+)$ state in ^{93}Rh (the respective 622 keV γ ray is observed in coincidence with protons and 511 keV γ rays only) in comparison with the strongly fed $(7/2^+)$ and $(11/2^+)$ levels. Such a difference can tentatively be understood as a preferable emission of protons with $\ell=2$, $j=5/2$ from the 6^+ and 8^+ states in ^{94}Pd while the $(5/2^+)$ level can be populated via emission of $\ell=4$, $j=9/2$ protons, this mode being suppressed by the much higher centrifugal barrier. The suggested interpretation gives one more evidence in favor of the spin-parity assignment (7^+) for the first isomer of ^{94}Ag.

The excitation energy of 6.3 MeV predicted for the (21^+) isomer by shell-model calculations [4] is in qualitative agreement with the obtained low-limit value of 5.4 MeV. At this high excitation energy, the (21^+) isomer is expected to be unbound to several exotic decay modes, such as direct (or Coulomb-delayed) one proton, two-proton or α emission to the ground state of the respective daughter nuclei: ^{93}Pd, ^{93}Rh and ^{90}Rh. The Q values estimated for these disintegration modes are 5.4, 1.8, and 3.8 MeV, respectively [5]. Such decays suffer from a strong angular-momentum hindrance, whereas transitions to highly excited high-spin states in the daughter nuclei have presumably small or negative Q values. Therefore, the branching ratio of the (21^+) isomer for direct charged-particle radioactivity should be very small. In addition, β-delayed two-proton and three-proton emissions from the ^{94}Ag isomers can be investigated. Due to the high centrifugal barrier, all the listed decay modes may result in the excited states of the daughter nuclei ^{93}Pd, ^{92}Rh, ^{92}Ru, ^{91}Tc, and therefore may be followed by corresponding γ deexcitations. However, none of the γ rays from the low-lying states of the nuclei mentioned above has been observed neither in proton-γ nor in proton-γ-γ events. The detailed report of the search for direct particle emission will be published elsewhere [27].

At last, we would like to note that the super allowed Fermi decay of the 0^+ ground state of ^{94}Ag, with a half-life of 29^{+29}_{-10} ms [2], has not been observed in this work. This is apparently related to the fact that the heavy-ion induced fusion–evaporation reactions such as ^{58}Ni(^{40}Ca, $p3n$) prefer-

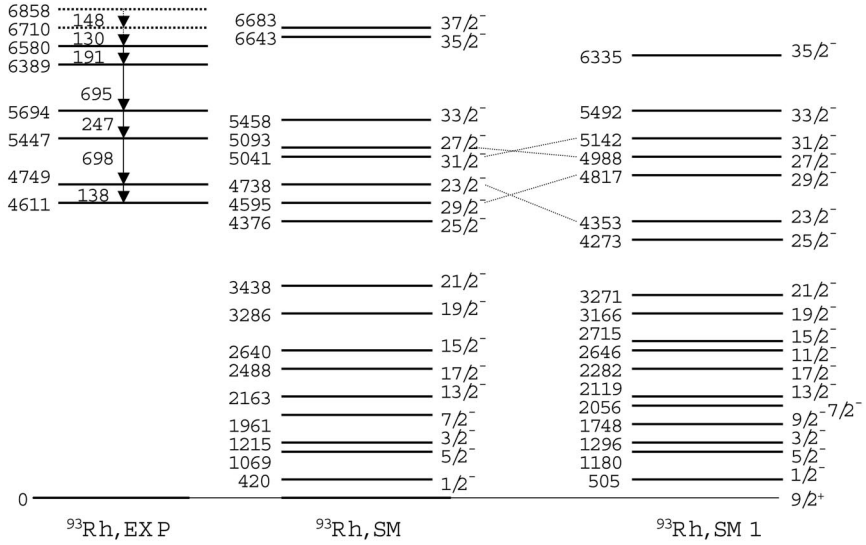

FIG. 10. Odd-parity yrast states in ^{93}Rh. Shell-model predictions (center and right panels) are shown together with the experimental scheme derived from the proton-γ data (left panel).

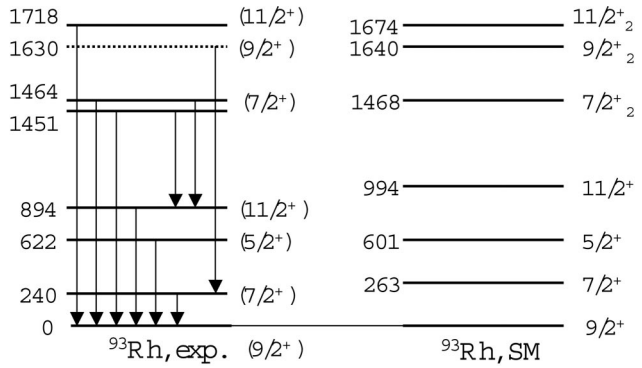

FIG. 11. Low-excitation energy states in ^{93}Rh resulting from shell-model calculations (right panel) are shown in comparison with the experimental scheme derived from the γ rays observed in β decay of ^{94}Ag in coincidence with delayed protons (left panel).

ably populate high-spin states. Correspondingly, the (7^+) and (21^+) isomers receive the major share of the ^{58}Ni(^{40}Ca, $p3n$) cross section and, in the absence of major internal branches of their deexcitation, "block" the population of the ground state in this reaction. Contributions of the ground state of ^{94}Ag to the mass-separated $A=94$ beam are further suppressed due to the delay occurring in ISOL ion sources.

V. SUMMARY AND OUTLOOK

We have studied in detail the decay properties of the isomers in ^{94}Ag by measuring β^+/EC-delayed γ rays, protons, proton-γ and proton-γ-γ coincidences as well as β-strength distribution. The applied detection techniques have supplied a detailed spectroscopic information. In particular, the method of γ ray spectroscopy using coincident β-delayed protons was allowed to measure the decay branching ratios as small as 3×10^{-3}.

In addition to the known (7^+) isomer in ^{94}Ag, the (21^+) isomer with $T_{1/2}=0.39(4)$ s has been observed. The (21^+) excitation energy and Q_{EC} values were measured to be at least 5.4 and 17.7 MeV, respectively. This relatively long-lived state has presumably the highest spin ever observed for β-decaying nuclei. The delayed proton emission from the β^+/EC decay of the (21^+) isomer, has the branching ratio of 27% and results in a population of dozens of high-spin (up to 39/2) states in the daughter nucleus ^{93}Rh. The properties of the experimentally identified ^{93}Rh levels are compared to shell-model predictions. The simple $(p_{1/2},g_{9/2})$ configuration space describes well the ^{93}Rh even-parity yrast states up to the highest energy and spin values, however it fails to reproduce the right order of high-spin odd-parity yrast states. The application of the large $g_{9/2}$, $p_{1/2}$, $p_{3/2}$, and $f_{5/2}$ space improves the situation though a quantitative description of the data still needs to be achieved.

The (21^+) isomer is estimated to be open to several exotic decay modes like direct one-proton, two-proton, or α-particle emission, and further search experiments for such exotic radioactivity may bring new exciting results.

ACKNOWLEDGMENTS

The authors thank W. Hüller and K. Burkard for their contributions in operating the GSI-ISOL facility. The help of I. Kojuharov (GSI), R. Schwengner, and W. Schulze (FZ Rossendorf) in preparing the Ge-detector array is gratefully appreciated. One of the authors (Z.J.) acknowledges the support from the Polish Committee of Scientific Research under Grant No. KBN 2 P03B 035 23.

[1] K. Schmidt *et al.*, Z. Phys. A **350**, 99 (1994).
[2] A. Stolz *et al.*, in *Proceedings International Workshop on Selected Topics on N=Z Nuclei (PINGST 2000), Lund, Sweden, 2000*, edited by D. Rudolph and M. Hellström (Lund University, Lund Institute of Technology, Lund, Sweden, 2000), LUIP 0003, p. 113.
[3] M. La Commara *et al.*, Nucl. Phys. **A708**, 167 (2002).
[4] C. Plettner *et al.*, Nucl. Phys. **A733**, 20 (2004).
[5] G. Audi, A. H. Wapstra, and C. Thibault, Nucl. Phys. **A729**, 337 (2003).
[6] J. Döring *et al.*, Phys. Rev. C **68**, 034306 (2003).
[7] I. Mukha *et al.*, AIP Conf. Proc. **681**, 209 (2003).
[8] I. Mukha *et al.*, Nucl. Phys. (2004) (in print).
[9] R. Kirchner, Nucl. Instrum. Methods Phys. Res. B **26**, 204 (1987).
[10] R. Kirchner, Nucl. Instrum. Methods Phys. Res. B **204**, 179 (2003).
[11] E. Roeckl *et al.*, Nucl. Instrum. Methods Phys. Res. B **204**, 53 (2003).
[12] J. Eberth *et al.*, Nucl. Instrum. Methods Phys. Res. B **369**, 135 (1997).
[13] J. Gerl *et al.*, Conference on Physics from Large γ ray Detector Arrays, Berkeley, USA, 1994 (LBL 35687, UC 413, 1994), p. 159.
[14] I. Mukha *et al.*, GSI Scientific Report 2002 p. 225; http://www-aix.gsi.de/annrep2002.
[15] M. Karny *et al.*, Nucl. Instrum. Methods Phys. Res. B **126**, 411 (1997).
[16] L. Batist *et al.*, Nucl. Phys. **A720**, 245 (2003).
[17] L. Batist *et al.*, GSI Scientific Report 2003, p. 11; http://www-aix.gsi.de/annrep2003.
[18] H. A. Roth *et al.*, J. Phys. G **21**, L1 (1995).
[19] W. Kurcewicz *et al.*, Z. Phys. A **308**, 21 (1982).
[20] K. Schmidt *et al.*, Eur. Phys. J. A **8**, 303 (2000).
[21] L. Batist *et al.* (unpublished).
[22] N. B. Gove and M. J. Martin, Nucl. Data Tables **10**, 205 (1971).
[23] B. A. Brown, A. Etchegoyen, and W. D. M. Rae, *Computer Code* OXBASH, *MSU-NSCL Report*, 1988, p. 524.
[24] R. Gross and A. Frenkel, Nucl. Phys. **A267**, 85 (1976).
[25] E. Caurier and F. Nowacki, Acta Phys. Pol. B **30**, 705 (1999).
[26] J. Sinatkas *et al.*, J. Phys. G **18**, 1377 (1992); **18**, 1401 (1992).
[27] I. Mukha *et al.* (unpublished).